CHEMISTRY OF MATERIALS

ARTICLE

pubs.acs.org/cm

Rod-Shaped Au−Pd Core−Shell Nanostructures

Wang Annan, Peng Qing, and Li Yadong*

Department of Chemistry, Tsinghua University, Beijing, 100084, People's Republic of China

Supporting Information

ABSTRACT: A series of anisotropic Au−Pd core−shell nanocrystals (NCs) have been synthesized by controlled overgrowth of Pd on preintroduced Au nanorods serving as seeds. Iodide ions can selectively adsorb on the {110} facets of Pd and change the final morphology of core−shell nanostructures. The overall morphology can be manipulated by changing the structure directing core or the amount H_2PdCl_4 introduced. These anisotropic nanostructures with adjustable exposure facets and sizes enrich the types of Au−Pd core−shell structures, while the mechanism discussing the formation process will provide useful information for the further investigation.

KEYWORDS: rod, Au−Pd, core−shell

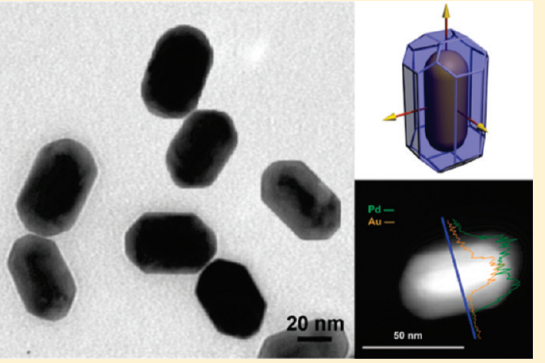

INTRODUCTION

Binary metallic nanocrystals (NCs) have received increasing interest, because their unique optical and catalytic properties can be easily tuned by controlling the size, shape and composition.[1−5] A seed-mediated method, using a presynthesized metal with a defined size and morphology for the further diffusion or deposition of another metal, has been proven to be an effective way for constructing a series of binary metallic NCs,[6−13] such as intermetallic compounds, hetero- or core−shell NCs. Based on our recent progress in Au−Cu intermetallic compounds[14] and Au−Co, Au−Ni heterostructures,[15] we further attempt using Au as the directing core to fabricate core−shell NCs for a systematic investigation on the binary metallic NCs. Most recently, much attention has been focused on the Au−Pd[16−21] core−shell NCs, since the complex electron interaction between the two electron-rich elements might give an enhancement to the catalytic efficiency of Pd,[12] leading to great potential applications in many Pd-catalyzed organic reactions. These previous works showed that the seed has great influence on the epitaxial growth of the deposited metal and then determines the structural and catalytic properties of the resultant nanostructures, so anisotropic materials, which are different from the isotropic seeds (such as cube and octahedron), also have great potential in constructing new classes of core−shell NCs with unusual morphologies and properties. However, it was a challenge to get rod-shaped core−shell nanostructures with a well-defined and easily manipulated overall morphology,[21−32] which is probably because the high-index {250}[33] or {037}[34] lateral facets of Au nanorods increased the difficulty in the further deposition of another metal.

In this work, Au nanorods were used as structure-directing cores for controlled deposition of Pd. By controlling the seed or growth environment, we get a series of anisotropic Au−Pd core−shell nanostructures via the seed-mediated method. Core−shell structure with different facts exposed can be obtained by involving I ions, and the overall morphology can be further manipulated by changing the structure-directing core or the Pd precursor that is introduced. These highly adjustable anisotropic nanostructures enrich the types of Au−Pd core−shell structures, while the mechanism discussing the formation process will provide useful information for further investigation.

EXPERIMENTAL SECTION

Chemicals and Reagents. $PdCl_2$ powder (Aldrich, 99%), hydrogen tetrachloroaurate trihydrate ($HAuCl_4 \cdot 3H_2O$, 99.9%, Aldrich), cetyltrimethylammonium bromide (CTAB, 98%, Beijing Chemical Factory of China), sodium borohydride ($NaBH_4$, 98%, Beijing Chemical Factory of China), ascorbic acid (AA, 99.7%, Beijing Chemical Factory of China), potassium iodide (KI, Beijing Chemical Factory of China), and hydrogen chloride (HCl, Beijing Chemical Factory of China) were used without further purification. Deionized water was used for all solution preparations.

Synthesis of Au Nanorods. Au nanorods were synthesized following the seed-mediated protocol developed by Nikoobakht and El-Sayed,[35] with some modification. More details are provided in the Supporting Information.

Synthesis of Au−Pd core−shell nanostructures. H_2PdCl_4 solution (0.01 M) was prepared by completely dissolving 0.089 g of $PdCl_2$ powder in 50 mL of 0.02 M HCl solution placed in a 60 °C water bath. In a typical synthesis of Au−Pd core−shell nanostructures using Au nanorods with an aspect ratio of AR = 2.5, 0.5 mL of a solution of Au nanorods, 0.2 mL of 0.01 M H_2PdCl_4 solution, and 0.15 mL of 0.01 M KI were added into 9.15 mL of 0.01 M CTAB solution sequentially. Then, 0.08 mL of 0.1 M ascorbic acid was added under stirring. The mixture

Received: April 11, 2011
Revised: May 26, 2011
Published: June 17, 2011

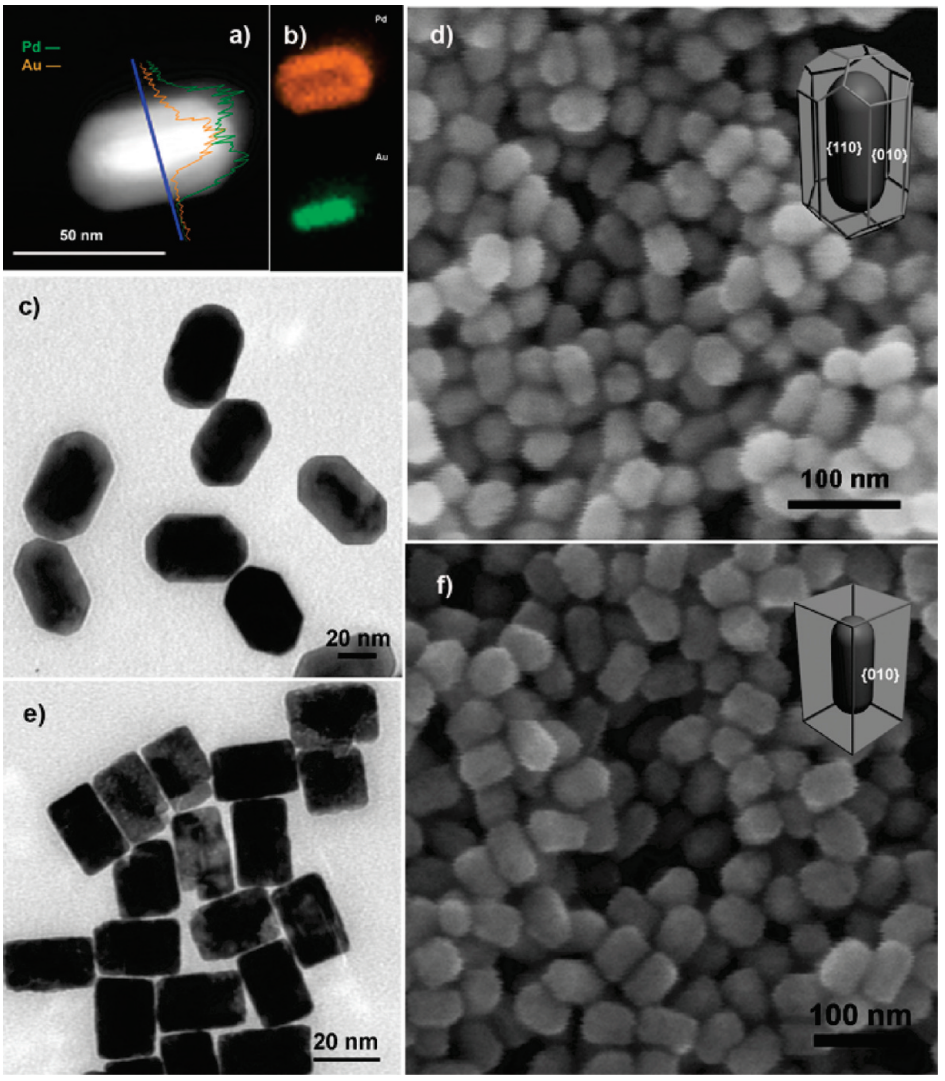

Figure 1. Truncated and cuboid Au-Pd core−shell nanocrystals (NCs), acquired when Au nanorods with an aspect ratio (AR) of 2.5 were serving as the structure-directing core: (a) HAADF-STEM image and the corresponding EDS line scan; (b) elemental mappings recorded on one truncated Au−Pd core−shell NC; (c) TEM image of truncated core−shell NCs; (d) SEM image of truncated core−shell NCs; (e) TEM image of cuboid Au-Pd core−shell NCs acquired when no KI was added; and (f) SEM image of cuboid Au-Pd core−shell NCs acquired when no KI was added. Insets in panels c and f are the corresponding models.

was kept in water bath set at 50 °C. After being left undisturbed for 2 h, the solution was centrifuged at 8500 rpm for 6 min. Tests that were conducted with no KI added while maintaining all the other parameters the same were used as control experiments.

In a typical synthesis of elongated tetrahexahedral (ETHH) Au−Pd core−shell NCs, 0.5 mL of tetrahexahedral (THH) Au nanorods solution, 0.1 mL of 0.01 M H_2PdCl_4 solution, and 0.5 mL of 0.1 M KI were added into 8.90 mL of 0.01 M CTAB solution sequentially. Then, 0.4 mL of 0.01 M ascorbic acid was added under stirring. The mixture was kept in a water bath set at 50 °C. After left undisturbed for 1 h, the solution was centrifuged at 4000 rpm for 6 min. Tests that were conducted with no KI added while maintaining all the other parameters the same were used as control experiments.

Au−Pd core−shell NCs with different shell thicknesses were prepared by setting the volume of H_2PdCl_4 introduced at 0.15 and 0.3 mL.

Characterization. The size and shape of the products were determined using transmission electron microscopy (TEM) (JEOL, Model JEM 1200EX, oeprating at 100 kV), scanning electron microscopy (SEM), and high-resolution transmission electron microscopy (HRTEM) (FEI Tecnai G2 F20 S-Twin, operating at 200 kV).

RESULTS AND DISCUSSION

Formation of Rod-Shaped Au−Pd Core−Shell Nanostructures with Different Facts Exposed. For a typical synthesis of rod-shaped Au−Pd core−shell nanostructures, using Au nanorods with aspect ratio (AR) of 2.5 (see Figures S1a and S1b in the Supporting Information) as the seeds, certain amounts of H_2PdCl_4 and KI were introduced into an aqueous CTAB solution of presynthesized Au nanorods. After ascorbic acid was added, Pd ions were gradually reduced and preferentially deposited on the preintroduced Au nanorods. TEM and SEM images in Figure 1c and 1d show the overall morphology of the products. HRTEM was conducted to further investigate the structural and elemental characters. One was selected randomly from the uniform particles and was characterized under different

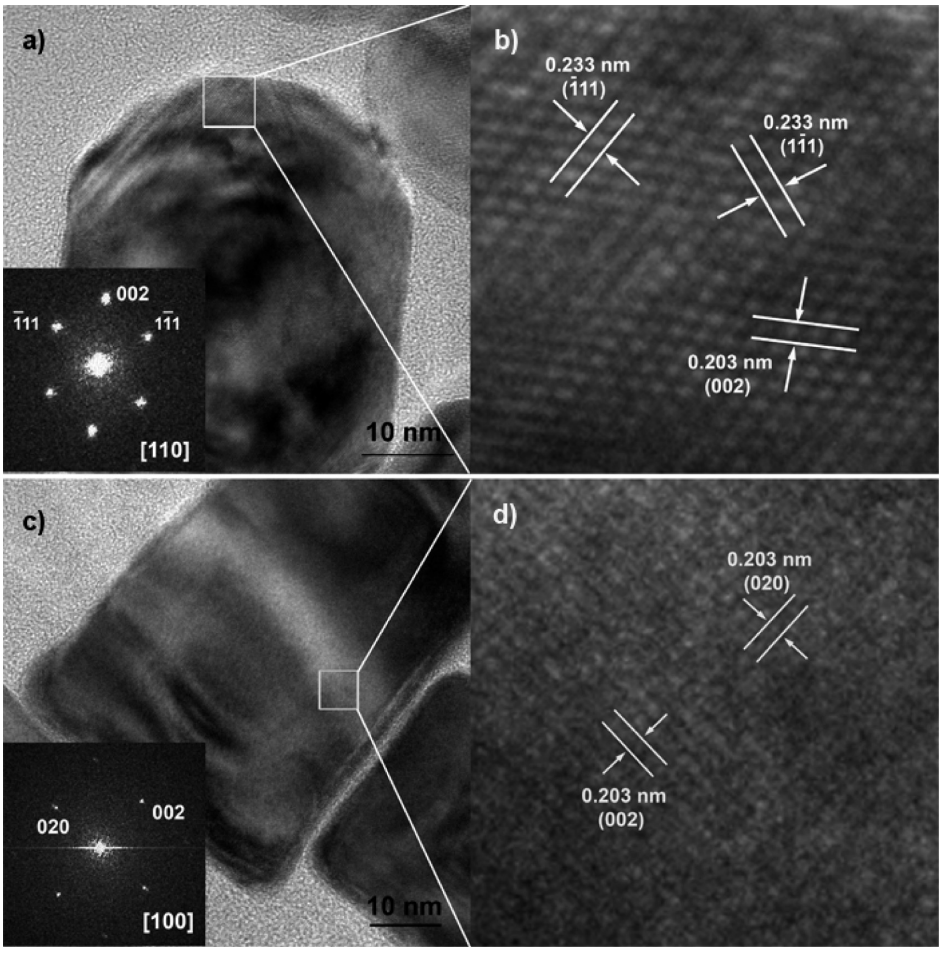

Figure 2. (a) HRTEM image of a truncated Au−Pd core−shell nanocrystal. (The inset shows the corresponding fast Fourier transform (FFT) pattern.) (b) HRTEM image of the region indicated with a box in panel a. (c) HRTEM image of a cuboid Au−Pd core−shell nanocrystal. (The inset is the corresponding FFT pattern.) (d) HRTEM image of the region indicated with a box in panel c.

modes of the HRTEM. EDS line scans and elemental mappings (see Figures 1 a and 1b) reveal that the rod-shaped nanostructure was composed of an Au core and a Pd shell. High-angle annular dark-field scanning transmission electron microscopy (HAADF-STEM) (Figure 1a), which shows the contrast in the central and outer region, further confirms that the nanocrystal adopts a core−shell structure. UV−vis−NIR spectra (see Figure S2 in the Supporting Information) show completely quenching of the characteristic absorption at 510 and 680 nm, demonstrating that Au nanorods have been completely encapsulated by the Pd layer. It is necessary to mention that the TEM image in Figure 1c clearly shows that a corner of the rectangle projection is truncated, which is quite different from the cuboid nanostructures prepared in the absence of KI (see Figure 1e). The shell measures ∼10 nm. The SEM image in Figure 1d also shows that the NCs are slightly truncated in the ends and have more than four facets in the lateral parts. They are highly monodisperse and are synthesized in high yield.

Interestingly, with all the other parameters the same except that no KI was added, resultant core−shell nanostructures adopt a cuboid shape with sharp corners (see Figures 1e and 1f). HRTEM characterization (see Figure 2) was conducted to further investigate the crystallographic properties of these two core−shell nanostructures, as shown in Figure 2. The clear Moire fringes and split points in the corresponding fast Fourier transform (FFT) pattern in both samples demonstrate their common single-crystalline nature of the shell. First, we consider the case of a truncated core−shell structure. A lattice distance of 0.203 nm corresponds to {002} facets of face-centered cubic (fcc) Pd NCs, whereas a lattice distance of 0.233 nm corresponds to {111} facets. Thus, the electron beam is aligned in the [110] direction, which indicates that the direction along the long axis is [001]. Then, we come to the case of cuboid ones. The two perpendicular sets of measured facets turn out to be {002} and {020}, in accordance with only one set of diffraction patterns in Figure 2c (inset). The incident direction is [100], whereas the long axis also corresponds to [001]. Additional HRTEM characterizations were respectively conducted on other NCs, and they all show similar diffraction behaviors. In both cases, they show a single crystalline nature with continuous Moire fringes throughout. In addition, the Pd atoms pack preferentially along the [001] direction, in accordance with the one-dimensional growth along the [001] direction of Au nanorods, whose crystallographic character has been confirmed previously.[33] Combining the two reasons above, we can come to the conclusion that uniform epitaxial growth of Pd on the Au core has been attained via careful control of the growth environment (such as concentration, temperature, etc.). However, facets exposed on the two

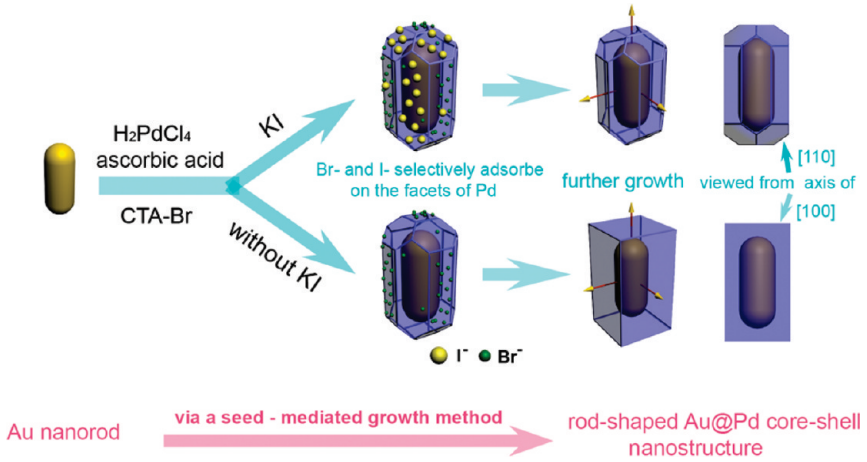

Figure 3. Schematic illustration of typical growth mechanisms for the formation of truncated and cuboid Au−Pd core−shell NCs using the seed-mediated method, in the presence or absence of I^- ions.

rod-shaped core−shell NCs are quite different, based on analysis of the corresponding FFT pattern. For truncated NCs, facets that are parallel to the carbon film thus perpendicular to the incident electron beam can be labeled as {110}. Since a notable proportion of NCs adopt such an orientation, we can conclude that at least some of the lateral facets are composed of the {110} facet. In addition, projection angles measuring 45° also suggest that corners are composed of {110} or {111} facets. Analyzing in the same way, cuboid structures are believed to be enclosed merely by {100} facets. These two can be illustrated as the models shown in Figures 1 d−f (inset). The truncated structure can be considered to evolve from a cuboid structure whose 12 edges (corresponding to the 12 [110] directions) are truncated thereafter, whereas the cuboid structure in Figure 2 well maintains its primary six faces (corresponding to the six [100] directions).

Since the addition of KI results in the distinction in overall morphology, these structural differences really provide us access to investigate the regulative role of I^- ions in the deposition process of Pd atoms. It has been demonstrated that halogen ions have special affinity with the surface of noble metals. In the case of Pd, Br^- anions from the CTAB are believed to have a stronger affinity with the {100} facets,[36,37] which inherits further deposition of newly reduced Pd atoms, so the growth rate of these facts is obviously slowed and these facets finally become dominant in the product. This is the formation process for cuboid core−shell NCs. However, when a certain amount of I^- ions is introduced, the situation changes. Previous reports showed that the I^- ions had a stronger affinity to the Pd surface than Cl^- ions. Therefore, it seems that the I^- ions will replace some of the Br^- ions on the surface of the Pd and selective interaction of I^- ions with different facets of Pd alters the surface energies of Pd. The exposure of {110} facets clearly demonstrates that I^- ions can stabilize the {110} facets of Pd and obviously improves the stableness of these facets. This agrees with the previous study[38] that investigated the regulation role of I^- ions in the synthesis of Pd NCs. Since the competitive growth of the three low-indexed facets can lead to a series of extreme and midst geometries,[19] it is reasonable to predict that rearrangement of the facet's energy in the presence of I^- ions assisting with the template-directing effect of Au nanorods can also lead to a series of one-dimensional truncated core−shell NCs. Two process that concern the formation process of the truncated and cuboid core−shell NCs are illustrated in Figure 3. This is more evidence proving the role of I^- ions when KI is absent. Even a relatively thin shell adopts a cuboid shape with merely {001} facets exposed (see Figures 5a−c, presented later in this paper), thus there exists a strong tendency to forming {001} facets in the CTAB system and this also demonstrates that I^- ions function in the earlier period of deposition. We also conducted control experiments by changing the concentration of CTAB. The core−shell structures adopt quasi-elliptical irregular shapes at higher concentrations of CTAB (see Figure S3 in the Supporting Information), suggesting that excessive adsorbents on the surface of the metal crystal will average their adsorption strength on different facets of the metal.

Formation of Au−Pd Core−Shell Nanostructures with Different Structure-Directing Cores or Different Shell Thicknesses. The dimension of the anisotropic Au−Pd core−shell nanostructures can be manipulated by changing the structure-directing core. Another type of Au nanorods, labeled as ETHH Au nanorods, whose high-indexed lateral facets has been confirmed by Ming et al,[34] were also used to prepare Au−Pd core−shell NCs, using the above-mentioned strategy with a slight change in the molar ratio of Au and Pd precursors, and, at the same time, the proper amount of I^- ions correspondingly. HAADF-STEM image and elemental mappings in Figures 4 c and 4d confirm their core−shell structure. TEM and SEM images (see Figures 4 a and 4b) show that the core−shell structures follow the shape of ETHH Au seeds, so they retain the ETHH shapes. A control experiment was conducted with no KI added while all the other parameters were kept the same. The results show obvious differences. The surfaces become flat and the overall shapes become more irregular, while high-index facets seem to disappear (see Figure S4 in the Supporting Information). Considering these two situations and the conclusions that we have drawn above, the role that I^- ions played can be explained as follows. Since I^- ions can adsorb onto certain facets of Pd and slow the growth rate of these facets and the overall growth rate of the shell, there will be enough time for the atoms to select the most suitable position on the preformed layer. Then, a uniform coating can be achieved. Since the shell thickness of the ETHH NCs is relatively thin, compared to the truncated structures mentioned above, the directing effects of the ETHH Au cores become dominant in the shell formation process, instead of the

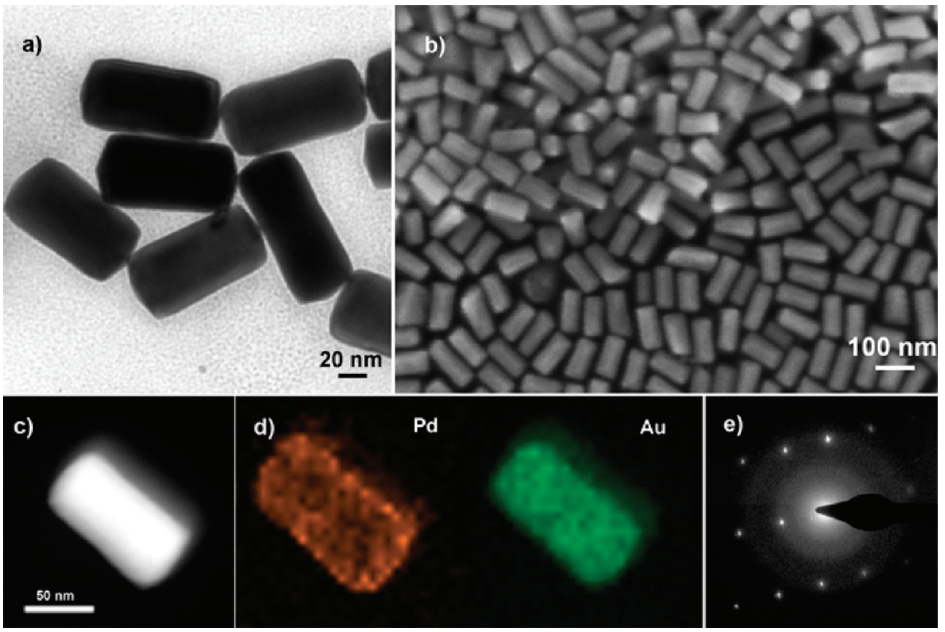

Figure 4. Au−Pd core−shell NCs acquired when ETHH Au nanorods were used as the structure-directing core: (a) TEM image, (b) SEM images, (c) HAADF-STEM image, (d) elemental mappings, and (e) electron-diffraction pattern recorded on the NC.

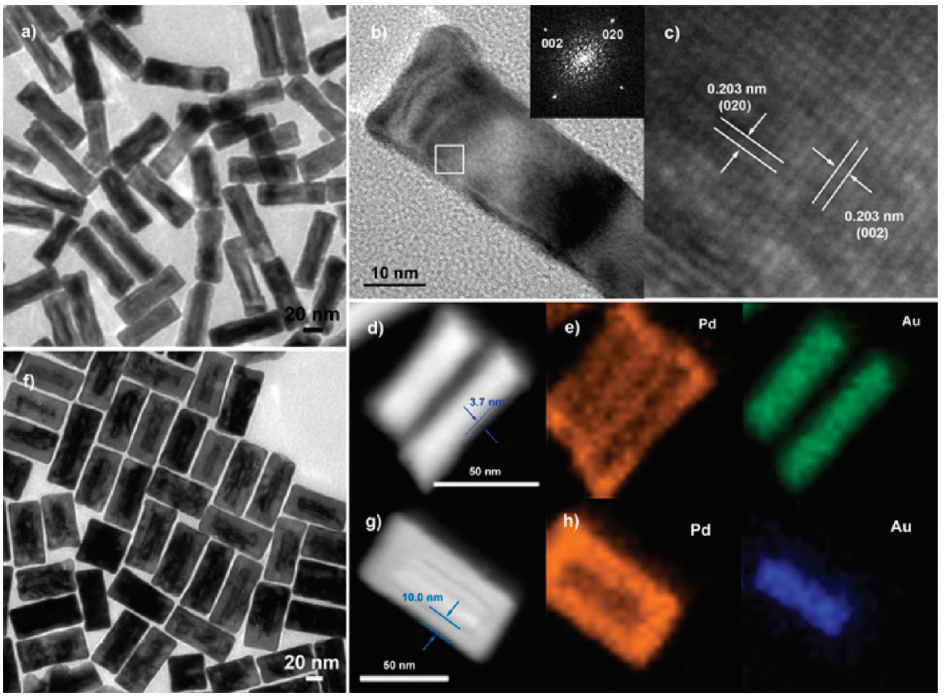

Figure 5. (a) TEM image of Au−Pd core−shell nanostructures with a thinner shell (∼3.7 nm). (b) HRTEM image of the Au−Pd core−shell NC in panel a. (Inset is the corresponding FFT pattern.) (c) HRTEM image of the region indicated with a box in panel b. (d) HAADF-STEM image of the Au−Pd core−shell nanostructure with a thinner shell. (e) Elemental mapping of the Au−Pd core−shell nanostructure with a thinner shell. (f) TEM image of a Au−Pd core−shell nanostructures with a thicker shell (∼10 nm). (g) HAADF-STEM image of the Au−Pd core−shell nanostructure with a thicker shell. (h) Elemental mapping of the Au−Pd core−shell nanostructure with a thicker shell.

growth environment. Then, the core−shell NCs adopt a perfect ETHH shape, following the inside cores.

Furthermore, the core−shell NCs show tunability in the shell thickness. The thickness is proportional to the amount of Pd precursor introduced to the system. More H_2PdCl_4 leads to a thicker shell. TEM images in Figures 5d and 5g show that the width grows from ∼3.7 nm to 10 nm, in accordance with the supplied amount of Pd precursor (in this case, Au nanorods with an aspect ratio of AR = 4.5 was used as the core (see Figures S1c and S1d in the Supporting Information). However, when the

dx.doi.org/10.1021/cm201023b |*Chem. Mater.* 2011, 23, 3217–3222

volume was >0.3 mL, small cuboid particles appeared as impurities, which can be attributed to the self-nucleation of palladium. It is not difficult to understand: When the concentration of precursor is high, the number of Pd atoms reduced in unit volume also increases. They will have a strong tendency to burst into small Pd nuclei, the so-called self-nucleation process, as long as the concentration reaches a critical point that is related to the solution environment. The shell thickness can be adjusted continuously within a certain range, depending on the practical requirements.

CONCLUSION

In summary, a series of anisotropic Au−Pd core−shell nanocrystals (NCs) have been synthesized via the controlled overgrowth of Pd on preintroduced Au nanorods, which serve as seeds. Especially, core−shell NCs with merely {001} or {110} and {001} facets exposed were selectively synthesized, depending on the regulation role of I^- ions. They can selectively adsorb on the {110} facets of Pd and change the relatively growth rate of the three low-indexed facets, then leading to the exposure of both {110} and {111} facets; whereas, in the absence of KI, only {100} facets become dominant in the final product. Investigation on the elongated tetrahexahedral (ETHH) Au−Pd core−shell NCs showed that I^- ions can also slow the reducing rate of the Pd precursor, leading to a more uniform coating. The overall morphology can be manipulated by changing the structure-directing core or the amount of H_2PdCl_4 introduced. These nanostructures add members to the Au−Pd core−shell family while the investigation on the formation process will provide useful information for the further exploration. In addition, these anisotropic Au−Pd core−shell NCs, involving an electron enhancement Au base as well as adjustable exposure facets and sizes, have potential application in catalyzing many organic reactions, such as Suzuki coupling reaction, oxidation of formic acid, etc.

ASSOCIATED CONTENT

Supporting Information. Experimental procedures, UV−vis-NIR, and additional TEM and SEM images. This material is available free of charge via the Internet at http://pubs.acs.org.

AUTHOR INFORMATION

Corresponding Author
*E-mail: ydli@mail.tsinghua.edu.cn.

ACKNOWLEDGMENT

This work was supported by the State Key Project of Fundamental Research for Nanoscience and Nanotechnology (No. 2011CB932401) and the Foundation for Innovative Research Groups of the National Natural Science Foundation of China (Grant No. 20921001). We also thank Caiyun Nan, Yanran Cui, Deren Chu, and Lingling Li for their genuine help throughout the work.

REFERENCES

(1) Habas, S. E.; Lee, H.; Radmilovic, V.; Somorjai, G. A.; Yang, P. *Nat. Mater.* **2007**, *6*, 692.
(2) Wang, C.; Hou, Y.; Kim, J.; Sun, S. *Angew. Chem., Int. Ed.* **2007**, *46*, 6333.
(3) Lim, B.; Kobayashi, H.; Yu, T.; Wang, J.; Kim, M. J.; Li, Z.; Rycenga, M.; Xia, Y. *J. Am. Chem. Soc.* **2010**, *132*, 2506.
(4) Wang, D.; Peng, Q.; Li, Y. *Nano Res.* **2010**, *3*, 574.
(5) Tao, F.; Grass, M. E.; Zhang, Y.; Butcher, D. R.; Aksoy, F.; Aloni, S.; Altoe, V.; Alayoglu, S.; Renzas, J. R.; Tsung, C.; Zhu, Z.; Liu, Z.; Salameron, M.; Somoijai, G. A. *J. Am. Chem. Soc.* **2010**, *132*, 8697.
(6) Ataee-Esfahani, H.; Wang, L.; Nemoto, Y.; Yamauchi, Y. *Chem. Mater.* **2010**, *22*, 6310.
(7) Zhang, J.; Tang, Y.; Lee, K.; Ouyang, M. *Science* **2010**, *327*, 1634.
(8) Zhang, J.; Tang, Y.; Weng, L.; Ouyang, M. *Nano Lett.* **2009**, *9*, 4061.
(9) Ksar, F.; Laurence, R.; Keita, B.; Nadjo, L.; Beaunier, P.; Renita, H. *Chem. Mater.* **2009**, *21*, 3677.
(10) Peng, Z.; Yang, H. *Nano Res.* **2009**, *2*, 406.
(11) Ma, Y.; Li, W.; Cho, E. C.; Li, Z.; Yu, T.; Zeng, J.; Xie, Z.; Xia, Y. *ACS Nano* **2010**, *4*, 6725.
(12) Lee, H.; Habas, S.; Somorjai, G. A.; Yang, P. *J. Am. Chem. Soc.* **2008**, *130*, 5406.
(13) Wanjala, B. N.; Luo, J.; Loukrakpam, R.; Fang, B.; Mott, D.; Njoki, P. N.; Engelhard, M.; Naslund, H. R.; Wu, J. K.; Wang, L.; Malis, O.; Zhong, C. *Chem. Mater.* **2010**, *22*, 4282.
(14) Chen, W.; Yu, R.; Li, L.; Wang, A.; Peng, Q.; Li, Y. *Angew. Chem., Int. Ed.* **2010**, *16*, 2979.
(15) Wang, D.; Li, Y. *J. Am. Chem. Soc.* **2010**, *132*, 6280.
(16) Fan, F.; Liu, D.; Wu, Y.; Duan, S.; Xie, Z.; Jiang, Z.; Tian, Z. *J. Am. Chem. Soc.* **2008**, *130*, 6951.
(17) Lee, Y. W.; Kim, M.; Kim, Z. H.; Han, S. W. *J. Am. Chem. Soc.* **2009**, *131*, 17036.
(18) Jana, D.; Dandapat, A.; De, G. *J. Phys. Chem. C* **2009**, *113*, 9101.
(19) Lu, C.; Prasad, K. S.; Wu, H.; Ho, J. A.; Huang, M. H. *J. Am. Chem. Soc.* **2010**, *132*, 14546.
(20) Yu, Y.; Zhang, Q.; Liu, B.; Lee, J. Y. *J. Am. Chem. Soc.*, **2010**, *132*, 18258.
(21) Wang, F.; Li, C.; Sun, L.; Wu, H.; Ming, T.; Wang, J.; Yu, J. C.; Yan, C. *J. Am. Chem. Soc.* **2011**, *133*, 1106.
(22) Kim, Y.; Hong, J. W.; Lee, Y. W.; Kim, M.; Kim, D.; Yun, W. S.; Han, S. W. *Angew. Chem., Int. Ed.* **2010**, *122*, 10395.
(23) Grzelczak, M.; Perez-Juste, J.; de Abajo, F. J. G.; Liz-Marzan, L. M. *J. Phys. Chem. C* **2007**, *111*, 6183.
(24) Feng, L.; Wu, X.; Ren, L.; Xiang, Y.; He, W.; Zhang, K.; Zhou, W.; Xie, S. *Chem.—Eur. J.* **2008**, *14*, 9771.
(25) Khanal, B. P.; Zubarev, E. R. *Angew. Chem., Int. Ed.* **2009**, *48*, 6888.
(26) Cho, E. C.; Camargo, P. H. C.; Xia, Y. *Adv. Mater.* **2010**, *22*, 744.
(27) Sanchez-Iglesias, A.; Carbo-Argibay, E.; Glaria, A.; Rodriguez-Gonzalez, B.; Perez-Juste, J.; Pastoriza-Santos, I.; Liz-Marzan, L. M. *Chem.—Eur. J.* **2010**, 16.
(28) Huang, C.; Yang, Z.; Chang, H. *Langmuir* **2004**, *20*, 6089.
(29) Xiang, Y.; Wu, X.; Liu, D.; Li, Z.; Chu, W.; Feng, L.; Zhang, K.; Zhou, W.; Xie, S. *Langmuir* **2008**, *24*, 3465.
(30) Song, J. H.; Kim, F.; Kim, D.; Yang, P. *Chem.—Eur. J.* **2005**, *11*, 910.
(31) Grzelczak, M.; Rodríguez-González, B.; Pérez-Juste, J.; Liz-Marzán, L. M. *Adv. Mater.* **2007**, *19*, 2262.
(32) Xiang, Y.; Wu, X.; Liu, D.; Jiang, X.; Chu, W.; Li, Z.; Ma, Y.; Zhou, W.; Xie, S. *Nano Lett.* **2006**, *6*, 2290.
(33) Carbo-Argibay, E.; Rodriguez-Gonzalez, B.; Gomez-Grana, S.; Guerrero-Martinez, A.; Pastoriza-Santos, I.; Perez-Juste, J.; Liz-Marzan, L. M. *Angew. Chem., Int. Ed.* **2010**, *122*, 9587.
(34) Ming, T.; Feng, W.; Tang, Q.; Wang, F.; Sun, L.; Wang, J.; Yan, C. *J. Am. Chem. Soc.* **2009**, *131*, 16350.
(35) Nikoobakht, B.; El-Sayed, M. A. *Chem. Mater.* **2003**, *15*, 1957.
(36) Jin, M.; Liu, H.; Zhang, H.; Xie, Z.; Liu, J.; Xia, Y. *Nano Res.* **2011**, *4*, 83.
(37) Lim, B.; Jiang, M.; Tao, J.; Camargo, P. H. C.; Zhu, Y.; Xia, Y. *Adv. Funct. Mater.* **2009**, *19*, 189.
(38) Niu, W.; Zhang, L.; Xu, G. *ACS Nano* **2010**, *4*, 1987.